Intramyocellular Lipid Is Associated With Resistance to In Vivo Insulin Actions on Glucose Uptake, Antilipolysis, and Early Insulin Signaling Pathways in Human Skeletal Muscle

Antti Virkamäki,[1] Elena Korsheninnikova,[1] Anneli Seppälä-Lindroos,[2] Satu Vehkavaara,[2] Takashi Goto,[1] Juha Halavaara,[3] Anna-Maija Häkkinen,[4] and Hannele Yki-Järvinen[2]

To examine whether and how intramyocellular lipid (IMCL) content contributes to interindividual variation in insulin action, we studied 20 healthy men with no family history of type 2 diabetes. IMCL was measured as the resonance of intramyocellular CH_2 protons in lipids/resonance of CH_3 protons of total creatine (IMCL/Cr_T), using proton magnetic resonance spectroscopy in vastus lateralis muscle. Whole-body insulin sensitivity was measured using a 120-min euglycemic-hyperinsulinemic (insulin infusion rate 40 mU/m^2 · min) clamp. Muscle biopsies of the vastus lateralis muscle were taken before and 30 min after initiation of the insulin infusion to assess insulin signaling. The subjects were divided into groups with high IMCL (HiIMCL; 9.5 ± 0.9 IMCL/Cr_T, n = 10) and low IMCL (LoIMCL; 3.0 ± 0.5 IMCL/Cr_T, n = 10), the cut point being median IMCL (6.1 IMCL/Cr_T). The groups were comparable with respect to age (43 ± 3 vs. 40 ± 3 years, NS, HiIMCL versus LoIMCL), BMI (26 ± 1 vs. 26 ± 1 kg/m^2, NS), and maximal oxygen consumption (33 ± 2 vs. 36 ± 3 ml · kg^{-1} · min^{-1}, NS). Whole-body insulin-stimulated glucose uptake was lower in the HiIMCL group (3.0 ± 0.4 mg · kg^{-1} · min^{-1}) than the LoIMCL group (5.1 ± 0.5 mg · kg^{-1} · min^{-1}, $P < 0.05$). Serum free fatty acid concentrations were comparable basally, but during hyperinsulinemia, they were 35% higher in the HiIMCL group than the LoIMCL group ($P < 0.01$). Study of insulin signaling indicated that insulin-induced tyrosine phosphorylation of the insulin receptor (IR) was blunted in HiIMCL compared with LoIMCL (57 vs. 142% above basal, $P < 0.05$), while protein expression of the IR was unaltered. IR substrate-1–associated phosphatidylinositol (PI) 3-kinase activation by insulin was also lower in the HiIMCL group than in the LoIMCL group (49 ± 23 vs. 84 ± 27% above basal, $P < 0.05$ between HiIMCL and LoIMCL). In conclusion, IMCL accumulation is associated with whole-body insulin resistance and with defective insulin signaling in skeletal muscle independent of body weight and physical fitness. *Diabetes* 50:2337–2343, 2001

Abnormal lipid metabolism is a feature of the insulin resistance syndrome (1). In addition to an increase in the total amount of fat, the lipid disturbances include elevated circulating concentrations of triglycerides and free fatty acids (FFAs) (2) and an increase in visceral fat (3). Recently, several studies have shown an association between lipid accumulation in skeletal muscle and insulin resistance (4–10). In four of these studies, this relation was shown to be caused by intramyocellular rather than extramyocellular lipids, as measured by proton spectroscopy (5–7,11).

The causes for intramyocellular lipid (IMCL) accumulation are poorly understood. The first possibility is that IMCL is an innocent bystander and simply reflects overall adiposity. This is not supported by recent experiments in mice lacking subcutaneous fat, the A-ZIP/F-1 mice (12,13). These mice deposit fat intramyocellularly and exhibit severe insulin resistance, which is reversible by fat transplantation and rechanneling of IMCL back to subcutaneous depots. In humans, however, it is less clear whether IMCL is associated with insulin resistance independent of obesity. In 20 Europeans, Forouhi et al. (6) found the relationship between IMCL and insulin resistance to disappear after adjusting for obesity. In another study, no relation was found between IMCL and whole-body insulin sensitivity measured using the insulin tolerance test (4). In two other studies performed in relatives (7) or offspring (11) of type 2 diabetic patients, insulin resistance could not be attributed to obesity (7,11). Krssak et al. (5) found that IMCL did not correlate with insulin sensitivity, but in that study, both men and women were included and analyzed as one group. Because women appear to have more IMCL than men for the same BMI (11) but similar insulin sensitivity, despite greater adiposity (% body fat) than men with similar BMI (14), a lack of a correlation between IMCL and insulin sensitivity may have been confounded by the mixing of sexes.

Regarding the mechanisms by which IMCL could cause

From the [1]Minerva Foundation Institute for Medical Research, University of Helsinki, Helsinki; the [2]Department of Medicine, Division of Diabetes, University of Helsinki, Helsinki; the [3]Department of Radiology, University of Helsinki, Helsinki; and the [4]Department of Oncology, University of Helsinki, Helsinki, Finland.

Address correspondence and reprint requests to Antti Virkamäki, Minerva Foundation Institute for Medical Research, Biomedicum Helsinki, Haartmaninkatu 8, FIN-00290, Helsinki, Finland. E-mail: antti.virkamaki@hus.fi.

A.V. and E.K. contributed equally to this work.

Received for publication 26 January 2001 and accepted in revised form 13 July 2001.

CPT, carnitine palmityltransferase; Cr_T, CH_3 protons of total creatine; ECL, enhanced chemiluminescence; FFA, free fatty acid; HiIMCL, high intramyocellular lipid; IMCL, intramyocellular lipid; IMCL/Cr_T, resonance of intramyocellular CH_2 protons in lipids/resonance of Cr_T; IR, insulin receptor; IRS-1, IR substrate-1; LCACoA, long-chain fatty acid–CoA; LoIMCL, low IMCL; MR, magnetic resonance; MRI, MR imaging; PKC, protein kinase C.

insulin resistance, existing data suggest that an infusion of FFAs during hyperinsulinemia, but not under basal fasting conditions, acutely increases IMCL (15). This result seems physiologically feasible, given that FFAs appear to be transported in a concentration-dependent fashion into skeletal muscle, which has little need to oxidize FFAs under hyperinsulinemic conditions (16). In the studies mentioned above (4,6,7,11), FFAs were not determined during hyperinsulinemia to establish whether circulating FFAs are associated with IMCL in a chronic situation.

There are several potential intracellular mechanisms, in addition to the original glucose fatty-acid cycle theory proposed by Randle et al. (17), by which IMCL could impair insulin action. First, the mechanism could resemble that described for circulating FFAs. Acute elevation of serum FFAs causes whole-body insulin resistance, and a defect in the ability of insulin to normally activate insulin receptor substrate-1 (IRS-1)-associated phosphatidyl-inositol (PI) 3-kinase, a step that is important for insulin-stimulated glucose transport in skeletal muscle (18). Acute maintenance of FFAs during hyperinsulinemia by infusion of fat emulsion in rats has also been suggested to induce insulin resistance via overactivation of the hexosamine pathway (19). High-fat feeding in rats increases the concentration of long-chain acyl-CoA esters, which correlates with insulin sensitivity in humans (20) and directly inhibits activities of key enzymes, such as glycogen synthase (21), pyruvate dehydrogenase (16), and hexokinase (22).

In the present study, we determined *1*) whether IMCL is associated with insulin sensitivity not only independent of BMI, but also independent of other factors, such as $V_{O_{2max}}$ and visceral fat, as determined by magnetic resonance imaging (MRI); *2*) whether IMCL correlates with serum FFAs during hyperinsulinemia; and *3*) whether elevated IMCL is associated with defects in early insulin signaling, as has been described under conditions in which serum FFAs are increased.

RESEARCH DESIGN AND METHODS

Subjects and grouping. A total of 20 healthy men (42 ± 2 years), with a BMI ranging from 21 to 32 kg/m^2 (25.7 ± 0.7 kg/m^2, means ± SE) and no family history of type 2 diabetes, were studied on three occasions. On the first visit, IMCL content was measured using proton spectroscopy of the vastus lateralis muscle. On this visit, visceral and subcutaneous fat were also quantified using MRI. The subjects were divided into two groups: low IMCL (LoIMCL; 3.0 ± 0.5 resonance of intramyocellular CH_2 protons in lipids/resonance of CH_3 protons of total creatine [IMCL/Cr_T]) and high IMCL (HiIMCL; 9.5 ± 0.9 IMCL/Cr_T) based on their median IMCL content (6.1 IMCL/Cr_T). The LoIMCL and HiIMCL groups were comparable with respect to several parameters thought to cause insulin resistance (see RESULTS). On the second study occasion, maximal oxygen consumption ($V_{O_{2max}}$) was measured directly using an incremental bicycle ergometer test. On the third occasion, insulin sensitivity was measured using the euglycemic-hyperinsulinemic clamp technique. Before and after 30 min of insulin infusion, biopsies of the left and right vastus lateralis muscles were taken, respectively, for determination of early insulin signaling steps. All subjects were right-handed.

^{1}H-MR spectroscopy of IMCLs in muscle. Magnetic resonance (MR) images for localization and ^{1}H-MR spectroscopy were acquired using a 1.5 T MR system (Magnetom Vision; Siemens, Erlangen, Germany). A loop surface coil was used for detection. The subjects lay supine, with the left leg immobilized by firm padding. One-third of the distance from the trochanter major of the femur to the middle of the patella was measured, and the center of the coil was placed in contact with that spot. The ^{1}H-spectra were obtained from quadriceps femoris (vastus lateralis) muscle. The volume of interest, voxel (13 × 13 × 20 mm^3), was placed inside the lateral part of the vastus lateralis muscle to ensure parallel fiber orientation. The position of the voxel was chosen on the T_1-weighted MR images so that it did not contain any visible fat or fasciae known to contain significant amounts of adipocytes (23), which would affect the resonance-frequency shift data. Spatial localization was achieved by using a stimulated echo acquisition mode applied with a repetition time of 3,000 ms, with an echo time of 20 ms, and a mixing time of 30 ms. We used 128 excitations with water presaturation. The resonance at 1.5 ppm originates from the extramyocellular CH_2-protons of lipids (triglycerides and fatty acids) and the resonance at 1.3 ppm from intramyocellular CH_2-protons of lipids (23–25) (Fig. 1). Resonance intensities were expressed relative to the resonance at 3.0 ppm, which is derived from the CH_3-protons of total creatine (Cr_T; creatine and phosphocreatine). The spectral data were fitted in time domain with the program MRUI, based on the solving of nonlinear least squares problems (26). The IMCL data were quantified by using Cr_T signal intensity as a reference. The total water-to-Cr_T ratios were constant between subjects (signal intensity ratio 829 ± 46, correlation coefficient for signal intensity of water vs. Cr_T 0.96) and the Cr_T-to-water ratio (×10^4) averaged 12.9 ± 0.9 and 12.3 ± 1.2 in the LoIMCL and HiIMCL groups, respectively (NS). We chose IMCL/Cr_T for grouping criterion because both signals are of intramyocellular origin and of comparable magnitude of intensity (Fig. 1).

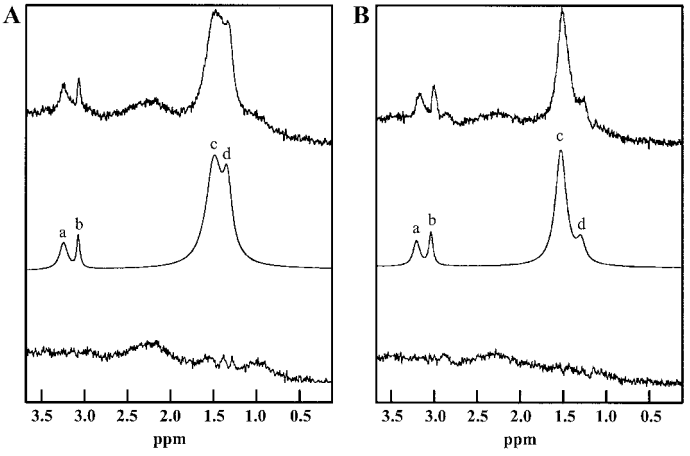

FIG. 1. Examples of spectral fitting using the MRUI program in subjects from the HiIMCL (*A*) and LoIMCL (*B*) groups (see RESEARCH DESIGN AND METHODS). The upper profiles in each panel show the experimental ^{1}H-spectrum (raw data). The middle profiles demonstrate the fitted spectrum using prior knowledge of (a) trimethyl-groups of total choline (3.2 ppm), (b) methyl-groups of total creatine (3.0 ppm), (c) CH_2-groups of EMCL (1.5 ppm), and (d) CH_2-groups of IMCL (1.3 ppm). The lower profiles show the difference spectrum (experimental–fitted profile).

Visceral and subcutaneous fat. A series of T1-weighted transaxial scans for the determination of visceral and subcutaneous fat were acquired from a region extending from 4 cm above to 4 cm below the 4th and 5th lumbar interspace (16 slices, field of view 375 × 500 mm^2, slice thickness 10 mm, and breath-hold repetition time divided by the echo time 138.9 ms/4.1 ms), as previously described (27). Visceral and subcutaneous fat areas were calculated using an image analysis program (available at www.perceptive.com/alice.htm). A histogram of pixel intensity in the intra-abdominal region was displayed, and the intensity corresponding to the nadir between the lean and fat peaks was used as a cut point. Visceral adipose tissue was defined as the area of pixels in the intra-abdominal region above this cut point. For calculation of subcutaneous adipose tissue area, a region of interest was first manually drawn at the demarcation of subcutaneous adipose tissue and visceral tissue.

Maximal aerobic power ($V_{O_{2max}}$). Maximal aerobic power was measured directly, using an incremental work-conducted upright exercise test with an electrically braked cycle ergometer (Ergometer Ergoline 900ERG; Ergoline GmbH, Bitz, Germany) combined with continuous analysis of expiratory gases and minute ventilation (Vmax 229 series; SensorMedics). Exercise was started at a workload of 50 W. The workload was then increased by 50 W every 3 min, until perceived exhaustion or a respiratory quotient of 1.10 was reached. Maximal aerobic power was defined as the V_{O_2} during the last 30 s of exercise.

Euglycemic-hyperinsulinemic clamp and muscle biopsies. After an overnight fast, whole-body insulin sensitivity was measured using a euglycemic-hyperinsulinemic clamp technique as previously described (28). Briefly, two indwelling catheters were inserted, one in an antecubital vein for infusion of insulin and glucose and another in a heated hand vein for sampling of arterialized venous blood. The rate of the continuous-rate insulin infusion was 40 mU/m^2 · min. The rate of the glucose infusion was adjusted to maintain euglycemia based on plasma glucose measurements that were performed every 5 min from arterialized venous blood.

TABLE 1
Basal characteristics of the study groups

	HiIMCL	LoIMCL	*P*
n	10	10	
Age (years)	43 ± 3	40 ± 3	NS
BMI (kg/m^2)	26 ± 1	26 ± 1	NS
Lean body mass (kg)	67 ± 3	64 ± 3	NS
fP-glucose (mmol/l)	5.8 ± 0.2	5.4 ± 0.1	NS
fS-insulin (pmol/l)	55 ± 10	38 ± 4	<0.05
Vo_{2max} (ml · kg^{-1} · min)	33 ± 2	36 ± 3	NS
fS-triglycerides (mmol/l)	1.6 ± 0.3	1.1 ± 0.2	<0.1
fS-cholesterol (mmol/l)	5.5 ± 0.3	5.0 ± 0.3	NS
fS-HDL-cholesterol (mmol/l)	1.3 ± 0.1	1.5 ± 0.1	NS
fS-free fatty acids (mmol/l)	0.63 ± 0.03	0.58 ± 0.05	NS

Data are means ± SE. f, Fasting; P, plasma; S, serum.

Muscle biopsies of vastus lateralis were obtained under local lidocaine anesthesia using a Bergström needle as previously described (29). Biopsies were frozen and stored in liquid nitrogen until analyzed. To minimize variability due to non–muscle tissue contaminants, such as blood, blood vessels, connective tissue, and fasciae and fat deposits, the muscle biopsy (~50 mg) was lyophilized (2–4 mbar, Edward freeze-dryer) for 14 h and macroscopically dissected free of nonmuscle contaminants using forceps and scalpel at room temperature conditions before homogenization.

Homogenization. Freeze-dried and purified muscle fibers (~10 mg) were homogenized (HETO, Birkerod, Denmark) for 2 min using a Teflon pestle in 1 ml of buffer A containing (in mmol/l) 25 Tris-HCl (pH 7.4), 10 sodium vanadate, 100 sodium fluoride, 10 sodium pyrophosphate, 10 EGTA, 10 ethylenediaminetetraacetic acid, one phenylmethylsulfonyl fluoride, and 5 μg/ml leupeptin, 5 μg/ml aprotinin, and 1% Nonidet P40. After centrifugation (275,000*g*, 1 h, plus 4°C) the supernatant was transferred to another tube, and its protein content was measured (BCA assay; Pierce, Rockford, IL).

Immunoprecipitation, Western blotting, and IRS-1–associated PI 3-kinase activity. To determine insulin receptor (IR) expression and IRS-1 associated PI 3-kinase enzymatic activity, the lysates were immunoprecipitated with an appropriate antibody (anti-IR or anti–IRS-1). Rotation with 40 μl of 50% protein A-Sepharose slurry (6MB) for 2 h at 4°C was used to trap the polyclonal antibodies. The beads were washed three times with buffer A and dried quickly. For detection of IR tyrosine phosphorylation and expression, 40 μl Laemmli's sample buffer was added, and the samples were boiled for 3 min, after which they were applied to SDS-PAGE (30). For IRS-1–associated PI 3-kinase detection, the dried samples were frozen and stored at −80°C before proceeding.

Immunoprecipitates stored at −80°C in Laemmli sample buffer were boiled for 3 min before protein separation by SDS-PAGE. After transferring the proteins to polyvinylidene difluoride membranes (Immobilon-P; Sigma, St. Louis, MO), the membranes were blocked using a 5% milk solution. Western blotting was performed using appropriate antibodies (against phosphorylated tyrosine [pY20] or IR) and enhanced chemiluminescence (ECL) detection. The films were scanned with a tabletop scanner and analyzed by using Image Gauge software (Version 3.12; Fuji Photo Film, Tokyo).

PI 3-kinase assay. The dried protein-A Sepharose beads stored at −80°C were washed twice with PI 3-kinase reaction buffer containing 20 mmol/l Tris-HCl, pH 7.4, 100 mmol/l NaCl, and 0.5 mmol/l EGTA and then dried quickly and resuspended in the same buffer supplemented with the PI 3-kinase substrate PI (Avanti Biolipids, Alabaster, AL), which was freshly suspended in 50 μl of PI 3-kinase reaction buffer by sonication for 10 min at 4°C. The PI 3-kinase reaction was initiated by the addition of 5 μl of $MgCl_2$-ATP mixture (200 mmol/l $MgCl_2$ and 200 μmol/l ATP) containing 5 μCi of [γ-^{32}P]ATP to the immunoprecipitates and incubated for 25 min at room temperature. The reaction was terminated by adding 150 μl of chloroform–methanol–11.6N HCl (100:200:2 dilution). After adding 120 μl of chloroform and 120 μl of methanol–1N HCl (1:1 dilution) twice, the organic phase was separated by centrifugation at 14,000 rpm for 1 min. The resulting organic phase was dried in SpeedVac (UVS400A; Savant Instruments, Holbrook, NY), dissolved in 15 μl of chloroform, spotted on a silica gel thin layer chromatography plate (Kieselgel 60; Merck, Darmstadt, Germany), and developed in chloroform–methanol–28% ammonium hydroxide–water (43:38:5:7 dilution) for 1 h. The phosphorylated products were visualized and quantified by a Bio-Imaging analyzer (BAS-5000; Fuji, Tokyo).

Materials. Polyclonal antibodies against IR (JD 15, JD 433) and IRS-1 (JD 288) were a gift from Professor C. Ronald Kahn (Joslin Diabetes Center, Harvard Medical School, Boston, MA). Horseradish-peroxidase rabbit anti–mouse antibodies, ECL kit, and [^{125}I]protein A and were from Amersham Pharmacia Biotech (Buckinghamshire, U.K.). The [γ-^{32}P]ATP was from NEN Research Products (Boston, MA). PI was from Avanti Polar Lipids (Alabaster, AL). Silica gel thin-layer chromatography plates were from Merck (Darmstadt, Germany). Immobilon-P transfer membranes were purchased from Millipore (Bedford, MA). Protein A-Sepharose 6MB was from Amersham Pharmacia Biotech (Uppsala, Sweden). Reagents for SDS-PAGE were from Bio-Rad (Richmond, CA). All other reagents were purchased from Sigma.

Analytical methods. Plasma glucose concentrations were measured in duplicate using the glucose oxidation method (Glucose Analyzer II; Beckman Instruments, Fullerton, CA) (31). Serum free insulin concentrations were determined by double-antibody radioimmunoassay (Insulin RIA Kit; Pharmacia, Uppsala, Sweden) after precipitation with polyethylene glycol. Serum FFAs were determined by the fluorometric method of Miles et al. (32), and serum triglycerides were determined by an enzymatic colorimetric assay (33) with an automated analyzer (Cobas Mira; F Hoffmann la Roche Diagnostica, Basel, Switzerland).

Calculations and statistical analysis. Whole-body insulin sensitivity was calculated from the glucose infusion rate needed to maintain euglycemia divided by body weight. Comparison of HiIMCL and LoIMCL groups was performed using Student's *t* test. For comparison of FFA concentrations between the groups, analysis of variance for repeated measures was used. Correlation coefficients were calculated using Pearson's correlation coefficient. All data are given as the means ± SE.

RESULTS

Characteristics of the study groups. The LoIMCL and HiIMCL groups were comparable with respect to age, BMI, and physical fitness (Table 1, Fig. 2). The groups also had similar volumes of visceral (3.4 ± 0.5 vs. 2.9 ± 0.3 l, LoIMCL versus HiIMCL, NS) and subcutaneous (2.9 ± 0.3 vs. 2.5 ± 0.5 l, NS) fat. The ratios of IMCL versus Cr_T were comparable between the HiIMCL (15 ± 4) and LoIMCL (17 ± 8, NS) groups. Plasma triglyceride concentrations were slightly higher in the HiIMCL group than in the LoIMCL group, but other lipid concentrations were comparable (Table 1.)

Insulin action on glucose and lipid metabolism. The fasting plasma glucose concentrations (Table 1) as well as the steady-state mean plasma glucose concentrations during the euglycemic-hyperinsulinemic clamp study (5.2 ± 0.1 vs. 5.2 ± 0.1 mmol/l, HiIMCL versus LoIMCL, NS) were comparable between the groups. The HiIMCL group had a

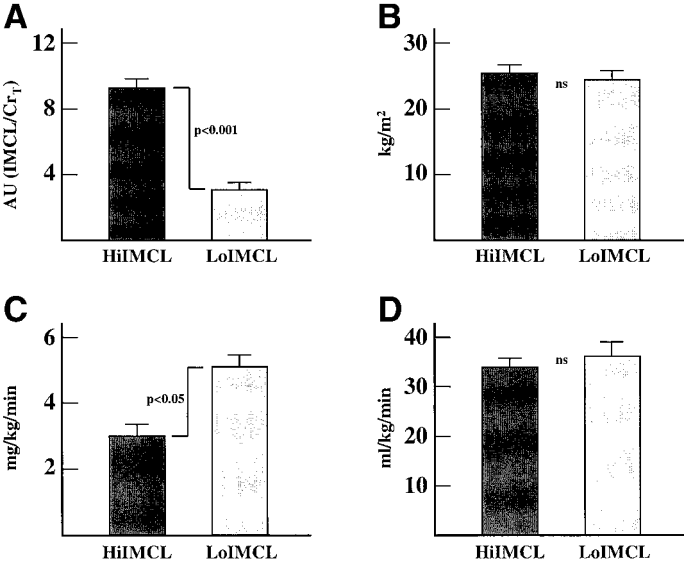

FIG. 2. IMCL content (*A*), BMI (*B*), insulin sensitivity (*C*), and maximal oxygen consumption (*D*) in LoIMCL and HiIMCL groups. NS, $P < 0.001$, and $P < 0.05$ refer to the statistical significance of the difference between the groups.

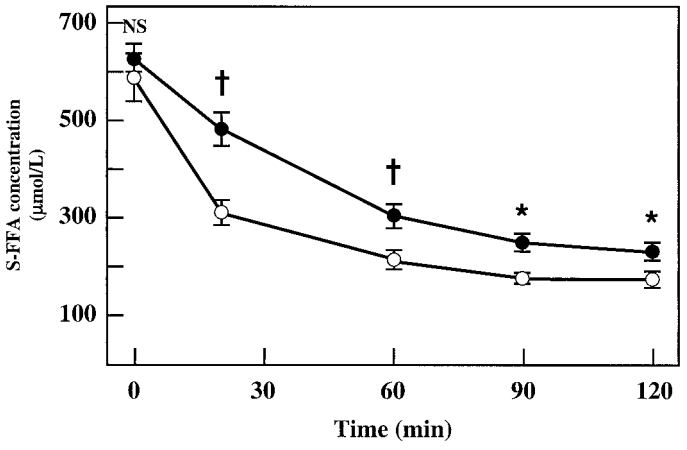

FIG. 3. Serum FFA concentrations in LoIMCL (○) and HiIMCL (●) groups during the euglycemic-hyperinsulinemic clamp study. *P < 0.05); †P < 0.01. NS and P values refer to the statistical significance of the difference between the groups at the given time point.

46% higher fasting insulin concentration (Table 1), and the insulin concentration remained slightly but significantly higher during the euglycemic-hyperinsulinemic clamp in the HiIMCL group (450 ± 24 vs. 382 ± 18 pmol/l, HiIMCL versus LoIMCL, $P < 0.05$), despite a similar insulin priming and infusion protocol. The serum insulin concentrations at the time of the muscle biopsy (30 min) were comparable between the groups (382 ± 26 vs. 340 ± 20 pmol/l, HiIMCL versus LoIMCL, respectively, NS).

Basally, before the insulin infusion, serum FFA concentrations were comparable between the groups (Table 1). During hyperinsulinemia, the FFA concentrations decreased slower (0.47 ± 0.04 vs. 0.31 ± 0.21 mmol/l at 20 min, HiIMCL versus LoIMCL, $P < 0.01$) and remained higher (0.23 ± 0.02 vs. 0.17 ± 0.02 mmol/l at 120 min) in the HiIMCL compared with the LoIMCL group (Fig. 3). IMCL was significantly correlated with serum FFA at all time points during the insulin infusion (data not shown) and with the mean FFA concentration during hyperinsulinemia ($r = 0.53$, $P < 0.02$) but not with the fasting FFA concentration ($r = 0.22$, NS).

The rate of glucose uptake expressed per body weight, fat-free mass, or body surface area was significantly lower in the HiIMCL compared with the LoIMCL group (3.0 ± 0.4 vs. 5.1 ± 0.4 mg/kg [total weight] · min, 3.8 ± 0.5 vs. 6.1 ± 0.5 mg/kg [fat-free mass] · min, $P < 0.005$; 124 ± 17 vs. 202 ± 16 mg/m^2 · min, $P < 0.005$; HiIMCL versus LoIMCL, $P < 0.005$) (Fig. 2). The correlation coefficient between IMCL and glucose uptake per body weight was −0.63 ($P < 0.01$).

IR tyrosine phosphorylation and PI 3-kinase activity. Insulin-induced IR tyrosine phosphorylation was determined using Western blotting from anti-IR immunoprecipitates after SDS-PAGE by determining the increase above basal phosphorylation in each subject. There were no detectable differences in the IR expression level by direct Western blotting from the tissue homogenates (data not shown). Normalized for respective protein expression level in each subject, the HiIMCL group had a blunted insulin–stimulated IR tyrosine phosphorylation (from 0.28 ± 0.07 to 0.44 ± 0.10, from basal to insulin-stimulated, respectively; NS) compared with the LoIMCL group (from 0.22 ± 0.08 to 0.55 ± 0.07, $P < 0.05$). The insulin-stimulated increase in tyrosine phosphorylation of the IR above basal was significantly blunted in the HiIMCL group (57 ± 7%) compared with the LoIMCL group (142 ± 8%, $P < 0.001$) (Fig. 4). The insulin-stimulated increase in the IRS-1–associated PI 3-kinase activity above basal activity was markedly decreased in the HiIMCL group (42 ± 13% above basal) compared with the LoIMCL group (88 ± 13% above basal, $P < 0.05$) (Fig. 4).

DISCUSSION

In the present study, we found two in vivo actions of insulin to be impaired in healthy men with a high content of IMCL (HiIMCL) compared with equally fit men with a similar BMI but a low content of IMCL (LoIMCL). Insulin-stimulated whole-body glucose uptake, which occurs primarily in skeletal muscle (34), was significantly blunted, as was the ability of insulin to decrease circulating FFA concentrations. Both insulin action on glucose and FFA metabolism were significantly correlated with IMCL independent of obesity, age, and physical fitness. We also measured early insulin signaling from vastus lateralis muscle biopsies taken before and after 30 min of in vivo hyperinsulinemia. Insulin stimulation of tyrosine phosphorylation of the IR and IRS-1–associated PI 3-kinase activity were significantly blunted in the HiIMCL group compared with the LoIMCL group.

The HiIMCL and LoIMCL groups had virtually identical BMIs and amounts of visceral and subcutaneous fat, as determined by MRI. This can be considered the first demonstration of an independent association between insulin sensitivity and IMCL in healthy subjects. This may be because previous studies either failed to separately quantitate intra- and extramyocellular fat (4,9,10,35), studied relatives (7) or offspring (11) of patients with type 2 diabetes, studied mixed sexes (5), or failed to find an independent association when BMI was included in the analysis (6). In the latter study, the number of subjects was similar, but the range of BMIs was greater than in the present study (6). The previous studies did not distinguish between intra- and extramyocellular fat, and obese subjects had higher muscle lipid contents than nonobese subjects in some (9,10) but not all (8) of those studies. Taken together, these data support the idea that IMCL can be related to insulin sensitivity independent of obesity, but also that obesity itself is associated with an increase in IMCL. Because the percentage of muscle that is lipid (extramycellular lipid plus IMCL) is ~1% in lean individuals and 2–3% in obese subjects (10), and because the IMCL

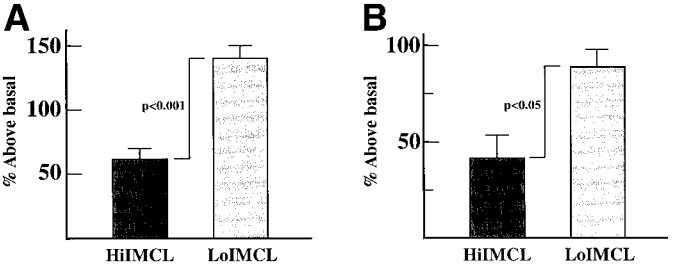

FIG. 4. The stimulatory effect of insulin on (*A*) IR phosphorylation normalized for protein expression and (*B*) IRS-1–associated PI 3-kinase activity. Data are expressed as the percent increase from basal (before insulin infusion). P values refer to the statistical significance of the difference between the groups.

component is usually smaller than the extramyocellular peak (25), variation in IMCL does not per se change total fat mass.

In addition to overall adiposity, fat distribution in visceral versus subcutaneous regions and physical fitness are established independent causes of variation of insulin sensitivity (36,37). Visceral and subcutaneous fat have previously been quantitated in one study in which a correlation was found between IMCL and measures of obesity, including BMI, percent fat, and visceral fat (6). In the present study, where an identical number of subjects were studied, such an association was not found, possibly because of a narrower range of obesity. During endurance exercise, muscle triglycerides represent an important source of energy. During low-intensity exercise, most of the oxidized fatty acids are derived from circulating fatty acids (38). During moderate-intensity exercise, the relative contribution of intramyocellular triglycerides increases and can represent nearly half of all fat that is oxidized (38). Physical training increases the capacity of muscle to oxidize fat (39) via mechanisms such as an increase in *1*) the density of mitochondria, *2*) the activities of respiratory enzymes, and *3*) the amount of carnitine palmityltransferase (CPT), which facilitates fatty acid transport across the mitochondrial membrane (40). These adaptations are opposite those found in obese human skeletal muscle, in which lipid oxidation (41), activities of muscle mitochondrial enzymes (42,43), and CPT-1 activity (41) are reduced. Data on IMCL levels are sparse but suggest, perhaps unexpectedly, that muscle triglyceride levels are similar or even higher in trained athletes than in sedentary control subjects (39,44–46). Electron microscopy studies have, however, revealed that the anatomical localization of lipid droplets within the myocyte differs between trained and untrained human subjects (47,48). In trained dogs, lipid droplets have been reported to surround and be in direct contact with mitochondria, whereas such an association is not observed in untrained animals (49). In sedentary subjects, lipid droplets may be located in the neutral lipid domains of the plasma membrane itself (47,48), which could interfere with membrane-associated signaling pathways, such as IR tyrosine phosphorylation. These data suggest that in addition to total IMCL content, study of the intramyocellular localization of fat might be of interest. Thus, although there was no correlation between $V\mathrm{O}_{2\mathrm{max}}$ and IMCL in our untrained subjects, a correlation might have been found between physical fitness and the amount of lipid localized in the mitochondrial compared with the plasma membrane compartment.

In the present study, both IR tyrosine phosphorylation and IRS-1–associated PI 3-kinase activation by insulin were significantly lower in the HiIMCL group than in the LoIMCL group. The defect in IRS-1–associated PI 3-kinase activity is similar to that recently found in fatless mice with a twofold increase in muscle triglycerides (12). In humans, an elevation of circulating FFA acutely, about fourfold above basal, decreases whole-body glucose uptake by 50% and abolishes insulin stimulation of IRS-1–associated PI 3-kinase activity (18). IR tyrosine phosphorylation was not measured in these two studies. The present data imply that regardless of whether FFAs originate from intramyocellular triglycerides or from the circulation, they may similarly influence early insulin signaling events. In the present study, the concentration of serum FFAs during hyperinsulinemia, but not under fasting conditions, was significantly correlated with IMCL. This finding is consistent with acute FFA infusion studies in which IMCL increased during hyperinsulinemia but not under basal conditions, perhaps because the combined effects of increased FFA availability and increased inhibition of intramyocellular lipolysis by insulin favor IMCL accumulation (15). It is thus possible that insulin resistance of lipolysis in adipose tissue or other sites, which contribute to circulating FFA, may be responsible for IMCL accumulation. On the other hand, because FFA fluxes were not quantitated in the present study, it is also possible that impaired insulin stimulation of FFA uptake in skeletal muscle or adipose tissue (50) was responsible for the higher FFA levels during hyperinsulinemia in the HiIMCL group compared with the LoIMCL group. Whether it is IMCL or circulating FFA that causes the signaling defects, or whether the signaling defects precede lipid accumulation, cannot be determined in a cross-sectional study.

Several possible mechanisms could link IMCL or circulating FFA to impaired insulin signaling. These include activation of signaling cascades known to downregulate either IR tyrosine phosphorylation or IRS-1 association with PI 3-kinase, such as activation of the hexosamine pathway (51), various protein tyrosine phosphatases (52), or protein kinase C (PKC) (53). The hexosamine pathway can be activated by infusion of either lipid or glucosamine (19). Both agents also decrease IRS-1–associated PI 3-kinase activity (18,51). Activation of the hexosamine pathway also increases *O*-glycosylation of IRS-1 (51), which may reduce IRS-1 phosphorylation and association with PI 3-kinase, but whether the effect of FFAs on the hexosamine pathway is important in mediating FFA-induced alterations in early insulin signaling and glucose uptake is not known and requires more definite experiments. Finally, it is also possible that increases in metabolites, such as malonyl-CoA (54) and long-chain fatty acid–CoA (LCACoA), may mediate effects of increased lipid availability on glucose metabolism and early insulin signaling. Infusion of FFA in rats increases muscle LCACoA (55). This increase has been suggested to increase PKC θ, a serine/threonine kinase, which is associated with decreased tyrosine and increased serine phosphorylation of IRS-1 (56). However, in humans, PKC θ is lower in obese subjects than in lean subjects (57). LCACoA may also interact directly with glucose metabolism through the inhibition of enzymes such as glycogen synthase (21) and hexokinase (22).

In summary, IMCL appears to be a feature of insulin resistance in skeletal muscle, which is associated with insulin resistance of antilipolysis and with signaling defects similar to those found to be acutely induced by infusion of FFA. It is unclear at present to what extent FFA derived from intra- versus extramyocellular sources regulate insulin signaling. If IMCL is important, it is an attractive therapeutic target because total myocellular lipid can be altered by weight loss (58), a low fat diet (46), and exercise (59,60). Although these manipulations may also change insulin sensitivity by mechanisms other than IMCL,

it is of interest that drugs such as troglitazone in Zucker diabetic fatty rats prevent overexpression of genes such as the sterol regulatory element–binding protein-1c (SREBP-1c; a lipogenic transcription factor) and ectopic fat accumulation, insulin resistance, and diabetes, despite increasing body weight and fat mass (61).

ACKNOWLEDGMENTS

This study was supported by grants from the Sigrid Juselius Foundation (to A.V. and H.Y.-J.), Liv och Hälsa (to A.V.), the Academy of Finland (to E.K., S.V., and H.Y.-J.), and the Finnish Diabetes Research Foundation (to A.V.)

REFERENCES

1. DeFronzo RA, Ferrannini E: Insulin resistance: a multifaceted syndrome responsible for NIDDM, obesity, hypertension, dyslipidemia, and atherosclerotic cardiovascular disease. *Diabetes Care* 14:173–194, 1991
2. Howard BV: Insulin resistance and lipid metabolism. *Am J Cardiol* 84:28J–32J, 1999
3. Kelley DE, Thaete FL, Troost F, Huwe T, Goodpaster BH: Subdivisions of subcutaneous abdominal adipose tissue and insulin resistance. *Am J Physiol Endocrinol Metab* 278:E941–E948, 2000
4. Phillips DI, Caddy S, Ilic V, Fielding BA, Frayn KN, Borthwick AC, Taylor R: Intramuscular triglyceride and muscle insulin sensitivity: evidence for a relationship in nondiabetic subjects. *Metabolism* 45:947–950, 1996
5. Krssak M, Falk PK, Dresner A, DiPietro L, Vogel SM, Rothman DL, Roden M, Shulman GI: Intramyocellular lipid concentrations are correlated with insulin sensitivity in humans: a 1H NMR spectroscopy study. *Diabetologia* 42:113–116, 1999
6. Forouhi NG, Jenkinson G, Thomas EL, Mullick S, Mierisova S, Bhonsle U, McKeigue PM, Bell JD: Relation of triglyceride stores in skeletal muscle cells to central obesity and insulin sensitivity in European and South Asian men. *Diabetologia* 42:932–935, 1999
7. Jacob S, Machann J, Rett K, Brechtel K, Volk A, Renn W, Maerker E, Matthaei S, Schick F, Claussen CD, Haring HU: Association of increased intramyocellular lipid content with insulin resistance in lean nondiabetic offspring of type 2 diabetic subjects. *Diabetes* 48:1113–1119, 1999
8. Pan DA, Lillioja S, Kriketos AD, Milner MR, Baur LA, Bogardus C, Jenkins AB, Storlien LH: Skeletal muscle triglyceride levels are inversely related to insulin action. *Diabetes* 46:983–988, 1997
9. Manco M, Mingrone G, Greco AV, Capristo E, Gniuli D, De Gaetano A, Gasbarrini G: Insulin resistance directly correlates with increased saturated fatty acids in skeletal muscle triglycerides. *Metabolism* 49:220–224, 2000
10. Goodpaster BH, Thaete FL, Kelley DE: Thigh adipose tissue distribution is associated with insulin resistance in obesity and in type 2 diabetes mellitus. *Am J Clin Nutr* 71:885–892, 2000
11. Perseghin G, Scifo P, De Cobelli F, Pagliato E, Battezzati A, Arcelloni C, Vanzulli A, Testolin G, Pozza G, Del Maschio A, Luzi L: Intramyocellular triglyceride content is a determinant of in vivo insulin resistance in humans: a 1H–13C nuclear magnetic resonance spectroscopy assessment in offspring of type 2 diabetic parents. *Diabetes* 48:1600–1606, 1999
12. Kim JK, Gavrilova O, Chen Y, Reitman ML, Shulman GI: Mechanism of insulin resistance in A-ZIP/F-1 fatless mice. *J Biol Chem* 275:8456–8460, 2000
13. Gavrilova O, Marcus-Samuels B, Graham D, Kim JK, Shulman GI, Castle AL, Vinson C, Eckhaus M, Reitman ML: Surgical implantation of adipose tissue reverses diabetes in lipoatrophic mice. *J Clin Invest* 105:271–278, 2000
14. Yki-Jarvinen H: Sex and insulin sensitivity. *Metabolism* 33:1011–1015, 1984
15. Brechtel K, Dahl DP, Machann J, Bachmann OP, Wenzel I, Maier T, Claussen CD, Haring HU, Jacob S, Schick F: Fast elevation of the intramyocellular lipid content in the presence of circulating free fatty acids and hyperinsulinemia: a dynamic 1H-MRS study. *Magn Reson Med* 45:179–183, 2001
16. Kelley DE, Mandarino LJ: Fuel selection in human skeletal muscle in insulin resistance: a reexamination (Review). *Diabetes* 49:677–683, 2000
17. Randle PJ, Garland PB, Hales CN, Newsholme EA: The glucose fatty-acid cycle: its role in insulin sensitivity and the metabolic disturbances of diabetes mellitus. *Lancet* i:785–789, 1963
18. Dresner A, Laurent D, Marcucci M, Griffin ME, Dufour S, Cline GW, Slezak LA, Andersen DK, Hundal RS, Rothman DL, Petersen KF, Shulman GI: Effects of free fatty acids on glucose transport and IRS-1-associated phosphatidylinositol 3-kinase activity. *J Clin Invest* 103:253–259, 1999
19. Hawkins M, Barzilai N, Liu R, Hu M, Chen W, Rossetti L: Role of the glucosamine pathway in fat-induced insulin resistance. *J Clin Invest* 99:2173–2182, 1997
20. Ellis BA, Poynten A, Lowy AJ, Furler SM, Chisholm DJ, Kraegen EW, Cooney GJ: Long-chain acyl-CoA esters as indicators of lipid metabolism and insulin sensitivity in rat and human muscle. *Am J Physiol Endocrinol Metab* 279: E554–E560, 2000
21. Wititsuwannakul D, Kim KH: Mechanism of palmityl coenzyme A inhibition of liver glycogen synthase. *J Biol Chem* 252:7812–7817, 1977
22. Thompson AL, Cooney GJ: Acyl-CoA inhibition of hexokinase in rat and human skeletal muscle is a potential mechanism of lipid-induced insulin resistance. *Diabetes* 49:1761–1765, 2000
23. Boesch C, Kreis R: Observation of intramyocellular lipids by 1H-magnetic resonance spectroscopy. *Ann N Y Acad Sci* 904:25–31, 2000
24. Schick F, Eismann B, Jung WI, Bongers H, Bunse M, Lutz O: Comparison of localized proton NMR signals of skeletal muscle and fat tissue in vivo: two lipid compartments in muscle tissue. *Magn Reson Med* 29:158–167, 1993
25. Szczepaniak LS, Babcock EE, Schick F, Dobbins RL, Garg A, Burns DK, McGarry JD, Stein DT: Measurement of intracellular triglyceride stores by H spectroscopy: validation in vivo. *Am J Physiol* 276:E977–E989, 1999
26. de Beer R, van den Boogaart A, van Ormondt D, Pijnappel WW, den Hollander JA, Marien AJ, Luyten PR: Application of time-domain fitting in the quantification of in vivo 1H spectroscopic imaging data sets. *NMR Biomed* 5:171–178, 1992
27. Ryysy L, Hakkinen AM, Goto T, Vehkavaara S, Westerbacka J, Halavaara J, Yki-Jarvinen H: Hepatic fat content and insulin action on free fatty acids and glucose metabolism rather than insulin absorption are associated with insulin requirements during insulin therapy in type 2 diabetic patients. *Diabetes* 49:749–758, 2000
28. DeFronzo RA, Tobin JD, Andres R: Glucose clamp technique: a method for quantifying insulin secretion and resistance. *Am J Physiol* 237:E214–E223, 1979
29. Vuorinen-Markkola H, Koivisto VA, Yki-Jarvinen H: Mechanisms of hyperglycemia-induced insulin resistance in whole body and skeletal muscle of type I diabetic patients. *Diabetes* 41:571–580, 1992
30. Laemmli UK: Cleavage of structural proteins during the assembly of the head of bacteriophage T4. *Nature* 227:680–685, 1970
31. Kadish AH, Litle RL, Sternberg JC: A new and rapid method for the determination of glucose by measurement of rate of oxygen consumption. *Clin Chem* 14:116–131, 1968
32. Miles J, Glasscock R, Aikens J, Gerich J, Haymond M: A microfluorometric method for the determination of free fatty acids in plasma. *J Lipid Res* 24:96–99, 1983
33. McGowan MW, Artiss JD, Strandbergh DR, Zak B: A peroxidase-coupled method for the colorimetric determination of serum triglycerides. *Clin Chem* 29:538–542, 1983
34. Utriainen T, Nuutila P, Takala T, Vicini P, Ruotsalainen U, Ronnemaa T, Tolvanen T, Raitakari M, Haaparanta M, Kirvela O, Cobelli C, Yki-Jarvinen H: Intact insulin stimulation of skeletal muscle blood flow, its heterogeneity and redistribution, but not of glucose uptake in non-insulin-dependent diabetes mellitus. *J Clin Invest* 100:777–785, 1997
35. Goodpaster BH, Thaete FL, Simoneau JA, Kelley DE: Subcutaneous abdominal fat and thigh muscle composition predict insulin sensitivity independently of visceral fat. *Diabetes* 46:1579–1585, 1997
36. Krotkiewski M, Bjorntorp P, Sjostrom L, Smith U: Impact of obesity on metabolism in men and women: importance of regional adipose tissue distribution. *J Clin Invest* 72:1150–1162, 1983
37. Yki-Jarvinen H, Koivisto VA: Effects of body composition on insulin sensitivity. *Diabetes* 32:965–969, 1983
38. Horowitz JF, Klein S: Lipid metabolism during endurance exercise. *Am J Clin Nutr* 72:558S–563S, 2000
39. Jansson E, Kaijser L: Substrate utilization and enzymes in skeletal muscle of extremely endurance-trained men. *J Appl Physiol* 62:999–1005, 1987
40. Holloszy JO: Biochemical adaptations in muscle: effects of exercise on mitochondrial oxygen uptake and respiratory enzyme activity in skeletal muscle. *J Biol Chem* 242:2278–2282, 1967
41. Kim JY, Hickner RC, Cortright RL, Dohm GL, Houmard JA: Lipid oxidation is reduced in obese human skeletal muscle. *Am J Physiol Endocrinol Metab* 279:E1039–E1044, 2000
42. Raben A, Mygind E, Astrup A: Lower activity of oxidative key enzymes and smaller fiber areas in skeletal muscle of postobese women. *Am J Physiol* 275:E487–E494, 1998

43. Simoneau JA, Bouchard C: Genetic determinism of fiber type proportion in human skeletal muscle. *FASEB J* 9:1091–1095, 1995
44. Essen-Gustavsson B, Tesch PA: Glycogen and triglyceride utilization in relation to muscle metabolic characteristics in men performing heavy-resistance exercise. *Eur J Appl Physiol Occup Physiol* 61:5–10, 1990
45. Hurley BF, Nemeth PM, Martin WH, Hagberg JM, Dalsky GP, Holloszy JO: Muscle triglyceride utilization during exercise: effect of training. *J Appl Physiol* 60:562–567, 1986
46. Lithell H, Orlander J, Schele R, Sjodin B, Karlsson J: Changes in lipoprotein-lipase activity and lipid stores in human skeletal muscle with prolonged heavy exercise. *Acta Physiol Scand* 107:257–261, 1979
47. Sweet W, Schroeder F: Lipid domains and enzyme activity. In *Lipid Domains and the Relationship to Membrane Function*. Aloia RC, Curtain CC, Gordon LM, Eds. New York, Alan R. Liss, 1988, p. 17–42
48. Curtain CC, Gordon LM, Aloia RC: Lipid domains in biological membranes: conceptual development and significance. In *Lipid Domains and the Relationship to Membrane Function*. Aloia RC, Curtain CC, Gordon LM, Eds. New York, Alan R Liss, 1988, p. 1–15
49. Taylor CR, Hoppeler H, Kennedy C, Valenski T, Roberts TJ, Weyand P: High fat diet improves aerobic performance by building mitochondria (Abstract). *Physiologist* 37: 1994
50. Furler SM, Cooney GJ, Hegarty BD, Lim-Fraser MY, Kraegen EW, Oakes ND: Local factors modulate tissue-specific NEFA utilization: assessment in rats using ^{3}H-(R)-2-bromopalmitate. *Diabetes* 49:1427–1433, 2000
51. Patti ME, Virkamaki A, Landaker EJ, Kahn CR, Yki-Jarvinen H: Activation of the hexosamine pathway by glucosamine in vivo induces insulin resistance of early postreceptor insulin signaling events in skeletal muscle. *Diabetes* 48:1562–1571, 1999
52. Goldstein BJ, Ahmad F, Ding W, Li PM, Zhang WR: Regulation of the insulin signalling pathway by cellular protein-tyrosine phosphatases. *Mol Cell Biochem* 182:91–99, 1998
53. Kellerer M, Lammers R, Haring HU: Insulin signal transduction: possible mechanisms for insulin resistance. *Exp Clin Endocrinol Diabetes* 107:97–106, 1999
54. Ruderman NB, Saha AK, Vavvas D, Witters LA: Malonyl-CoA, fuel sensing, and insulin resistance. *Am J Physiol* 276:E1–E18, 1999
55. Ruderman NB, Saha AK, Vavvas D, Kurowski T, Laybutt DR, Schmitz-Peiffer C, Biden T, Kraegen EW: Malonyl CoA as a metabolic switch and a regulator of insulin sensitivity. *Adv Exp Med Biol* 441:263–270, 1998
56. Griffin ME, Marcucci MJ, Cline GW, Bell K, Barucci N, Lee D, Goodyear LJ, Kraegen EW, White MF, Shulman GI: Free fatty acid-induced insulin resistance is associated with activation of protein kinase C θ and alterations in the insulin signaling cascade. *Diabetes* 48:1270–1274, 1999
57. Itani SI, Zhou Q, Pories WJ, MacDonald KG, Dohm GL: Involvement of protein kinase C in human skeletal muscle insulin resistance and obesity. *Diabetes* 49:1353–1358, 2000
58. Kelley DE, Goodpaster B, Wing RR, Simoneau JA: Skeletal muscle fatty acid metabolism in association with insulin resistance, obesity, and weight loss. *Am J Physiol* 277:E1130–E1141, 1999
59. Straczkowski M, Kowalska I, Gorski J, Kinalska I: The effect of a single bout of exhaustive exercise on muscle carbohydrate and lipid metabolism in a rat model of type 2 diabetes mellitus. *Acta Diabetol* 37:47–53, 2000
60. Krssak M, Petersen KF, Bergeron R, Price T, Laurent D, Rothman DL, Roden M, Shulman GI: Intramuscular glycogen and intramyocellular lipid utilization during prolonged exercise and recovery in man: a 13C and 1H nuclear magnetic resonance spectroscopy study. *J Clin Endocrinol Metab* 85:748–754, 2000
61. Kakuma T, Lee Y, Higa M, Wang Z, Pan W, Shimomura I, Unger RH: Leptin, troglitazone, and the expression of sterol regulatory element binding proteins in liver and pancreatic islets. *Proc Natl Acad Sci U S A* 97:8536–8541, 2000